atmosphere

MDPI

Article

Gini Method Application: Indoor Radon Survey in Kpong, Ghana

Filomena Loffredo [1,2,3,*], Irene Opoku-Ntim [4], Doris Kitson-Mills [5] and Maria Quarto [1,2]

[1] Advanced Biomedical Sciences Department, University of Naples Federico II, 80131 Naples, Italy; maria.quarto@unina.it
[2] Radioactivity Laboratory, Advanced Metrological and Technological Services (CeSMA), University of Naples, 80138 Naples, Italy
[3] National Institute for Nuclear Physics (INFN), 80126 Naples, Italy
[4] National Nuclear Research Institute, Ghana Atomic Energy Commission, Accra GW-0373-819, Ghana; i.ontim@gaecgh.org
[5] Department of Radiography, University of Ghana, Accra GA-271-3093, Ghana; dsoppong@ug.edu.gh
* Correspondence: filomena.loffredo@unina.it

Abstract: In this study, the indoor radon concentrations map, starting from a sparse measurements survey, was realized with the Gini index method. This method was applied on a real dataset coming from indoor radon measurements carried out in Kpong, Ghana. The Gini coefficient variogram is shown to be a good estimator of the inhomogeneity degree of radon concentration because it allows for better constraining of the critical distance below which the radon geological source can be considered as uniform. The indoor radon measurements were performed in 96 dwellings in Kpong, Ghana. The data showed that 84% of the residences monitored had radon levels below 100 Bqm^{-3}, versus 16% having levels above the World Health Organization's (WHO) suggested reference range (100 Bqm^{-3}). The survey indicated that the average indoor radon concentration (IRC) was 55 $\pm$ 36 Bqm^{-3}. The concentrations range from 4–176 Bqm^{-3}. The mean value 55 Bqm^{-3} is 38% higher than the world's average IRC of 40 Bqm^{-3} (UNSCEAR, 1993).

Keywords: Kpong; indoor radon concentration; kriging; Gini index

Citation: Loffredo, F.; Opoku-Ntim, I.; Kitson-Mills, D.; Quarto, M. Gini Method Application: Indoor Radon Survey in Kpong, Ghana. *Atmosphere* **2022**, *13*, 1179. https://doi.org/10.3390/atmos13081179

Academic Editor: Tania Martellini

Received: 24 June 2022
Accepted: 23 July 2022
Published: 26 July 2022

1. Introduction

Humans have always been exposed to natural ionizing radiation, both as a general population and as workers [1–3]. It can come from both the Earth, in particular from the subsoil, like radon [4–7], and from space through cosmic rays [8,9]. One of the radioactive products of the ^{238}U decay series is radon (^{222}Rn, with a half-life of 3.8 days). It is a gaseous element that is odorless and colorless. In contrast to the outdoors, where radon is of little concern to human health because it is quickly diluted by air mixing, the exposure to indoor radon concentrations can be extremely high and harmful. Several studies have revealed the association between exposure to radon and lung cancer [10–14]. Indoor radon gas exposure accounts for a significant portion of the radiation dose received by the general population [15–18] in many nations, for both smokers and non-smokers. The geology of the area must be considered when assessing the danger of radon exposure because the soil is the main source of Rn. To effectively execute locally based risk reduction initiatives, thorough maps of indoor radon concentrations are needed. The most fundamental geostatistical procedures are based on two phases known as variogram fit and kriging [19], which are utilized in a variety of projects. The technique used to create the maps is determined by the spatial resolution required.

Simple Kriging (SK), Ordinary Kriging (OK), Universal Kriging, and CoKriging are the most commonly utilized methods in the literature (multivariate geostatistics). In addition, fractal and multi-fractal analysis, Bayesian spatial quantile regression, and classic

multivariate statistical techniques are also viable options for this type of analysis. [20–26]. Several factors influence indoor concentration measurements, which show significant variation. Applying interpolation techniques like kriging, for example, might be challenging because these techniques must be deployed after data pretreatment [27]. A new method for the realization of maps based on the calculation of the Gini index has recently been developed and shown [28–30]. It can tell the difference between variations generated by environmental influences and those caused by random spatially uncorrelated noise. The Gini index also provides for a more precise determination of the minimal distance beyond which the radon geological source may be deemed uniform, at least for the length scales of variability investigated [29]. The interpolated maps in this study were created using the Gini index.

With the voluntarily cooperation of the locals, the indoor radon measuring survey at the Kpong was made possible. The measurements were taken in 96 dwellings, all of which were on the ground floor; for this reason in the specific case, the radon concentration variability is independent of the floor, otherwise the data should be normalized [30]. Dependence on the floor is one of the determining factors in the estimates of radon concentration, as well demonstrated in the literature. Instead, a *t*-test was used to ensure that the concentrations were unaffected by the building materials, ensuring that there was no statistically significant difference between the concrete structures and the cement-plastered ones. The concluding section involved comparing the findings of this study to related research that was conducted at Aburi, which is located in the same region as Kpong, and presenting the findings of the Kpong study based on their geology. The aim of this work is the spatial link among radon readings using the mapping based on the Gini method (kriging).

Many countries have established a radon concentration action level to guide their radon management programs at home. Currently, in Ghana there is no national average for radon levels in dwellings. One of the reasons for no national law is insufficient data, hence the need for more indoor radon measurement across the country [17,18,31,32]. This work is being done as part of the national data collation and radon advocacy among the people of Kpong.

2. Materials and Methods

2.1. Kpong-Ghana

Kpong is one of the towns situated in the Lower Manya Krobo Municipality. The Municipality is located at the eastern corner of the Eastern Region of Ghana (see Figure 1) which lies between latitude 6.05 N and longitude 0.20 W with an altitude of 457.5 m above sea level. With a household population of 87.649 the Lower Manya Krobo Municipality has an average household size of four persons per household. The lower Manya Krobo municipality lies within the semi-equatorial climate belt with a mean annual rainfall ranging between 900 mm to 11.500 mm. The relative humidity is high during the wet season and low in the dry season. The Municipality experiences two major seasons; wet (from April to October) and dry (from November to March). Temperatures are generally high, ranging between 26 °C and 35 °C. The municipality falls under the influence of two wind systems: the southwest monsoon winds which blow from the Atlantic Ocean between March and July, and the northeast trade winds (harmattan) from the Sahara Desert which blow from November and early March [33]. The main construction material for the outer walls of dwelling units in the municipality is cement blocks/concrete, which account for 69.7%, with mud bricks/earth constituting 25.9% of the outer walls of dwelling units. Cement (86.8%) and mud/earth (10.1%) are the two main materials used in the construction of floors of dwelling units in the district. The main bedrock is the Togo formation (schists, quartzite and phyllites, unaltered shale and sandstone) forming the Akwapim range of hills trending northeast from the coast West of Accra through Kpong, Aburi, Anum, and into the Republic of Togo [34].

Figure 1. A map showing Kpong in Accra, Ghana (Latitude 6.160649° and Longitude 0.058329°).

2.2. Indoor Radon Measurements

Indoor measurements of ^{222}Rn are increasingly performed using SSNTDs, or solid state nuclear track detectors. Long-term observations of α activity in indoor radon, as well as large-scale surveys for many measurements at the same time, are possible with these small and inexpensive detectors. The measurement period, which can last anywhere from a few months to a year, reduces the impact of any short-term variations in ^{222}Rn concentration on the measurement results. To assess the indoor concentrations of ^{222}Rn in dwellings, the current study used Kodak-Pathe LR-115 Type II detectors (from Dosirad, France). The radon measurement device employed in the study used a self- made envelope inside which an LR-115 detector with dimensions of 3 cm $\times$ 2 cm was mounted. Figure 2 shows the self-made device is a paper holder that was made from a cardboard to hold the detector in place during measurement [17].

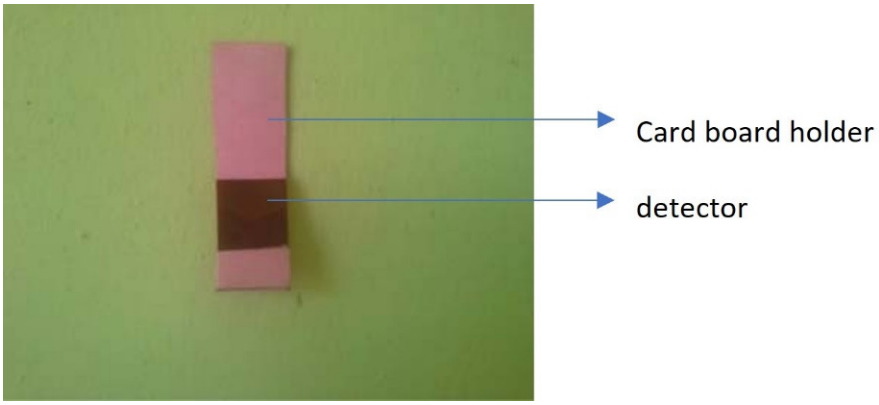

Figure 2. Self-made device deployed in the dwellings.

The Geographical Positioning System GPS was used to determine the location of dwellings where participants agreed to participate in the study (see Figure 3) [17,33]. SSNTD detectors in the bare mode were installed at a height of 1.65m from the floor level of the bedroom and/or the halls of families for a three-month period. The SSNTD was used

in the bare mode to determine radon as well as its progenies in the indoor environment. Ghana as a country is in the process of mapping its radon levels and associated progenies. Therefore, this method is part of the methods used in our mapping process.

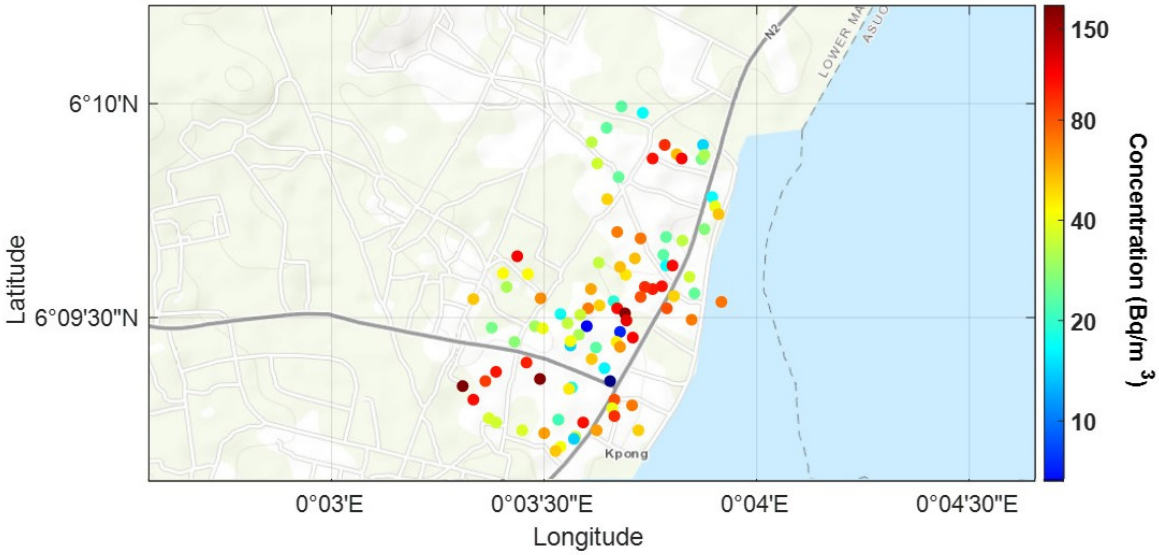

Figure 3. The GPS location of the dwellings of the participants that agreed to participate in the study in Kpong, Ghana.

Measurements were taken from September 2017–January 2018. The first measurements were from September 2017 to November 2017 and second measurements took place between November 2017 and January 2018. The environmental conditions within the measurement period was largely the same, since they were taken during the dry season in Ghana; the average temperature in the area is approximately 28 °C.

The detectors were recovered after the exposure and chemically etched in a 2.5 M NaOH solution. The solution was made by dissolving 100 g of NaOH pellets in 1 L of distilled water. The detectors were etched for 1 h and 30 min at a steady temperature of (60 °C). The detectors were rinsed for 20 min under running water to stop the etching process, then transferred to distilled water for 15 min before peeling and drying for track counting. For image processing and track counting, a commercial scanner (Epson Perfection V600) and ImageJ (Image Processing and Analysis in Java), a free digital image-processing software, was used. These procedures were performed at the Nuclear Track Detection Laboratory of the National Nuclear Research Institute (NNRI), Ghana Atomic Energy Commission (GAEC). The detectors used in this work were calibrated at the Radioactivity Laboratory in Italy. The radon concentration measurements in this study were carried out using a quality assurance system according to the UNI EN ISO 9001:2015 standard [17]. The radon concentration was calculated using Equation (1):

$$C_{Rn} = \frac{(\rho - \rho_B)}{(\varepsilon) \times (T)} \quad (1)$$

where, ρ is the track density that is the ratio between mean number of counts and area, ρ_B is background track density, ε = 3.96 Tracks m^3 /cm^2 kBq h is the Calibration Factor of the LR-115 (Type II) and T is the exposure time (h). The background track density was determined by counting the tracks of a significant number of unexposed detectors. The measurement uncertainty was determined using the metrological approach, taking into account the contribution of all terms. As a quality control, at every five measurement sites, two passive detectors (instead of just one) were placed to perform a duplicate test in order to estimate the uniformity of the reading.

3. Statistical Analysis

To determine the normality of the log-transformed data, the Kolmogorov–Smirnov test was used. The Statistical Package for the Social Sciences was used for all statistical analyses (IBM SPSS Statistic 27). A *t*-test was performed to verify the independence of radon concentrations from building materials.

Gini Index-Spatial Analysis

The most basic geostatistical approaches are based on two phases known as variogram fit and kriging [19]. The variogram gives a quantitative measure of a sparse dataset's spatial autocorrelation. Based on this autocorrelation, kriging can interpolate the given dataset, computing predicted values on a finer grid with a predefined resolution.

For discrete sampling, an empirical semi-variogram can computed as:

$$\gamma(h \pm \delta) = \frac{1}{2n(h \pm \delta)} \sum_{n(h \pm \delta)} \{z_i - z_j\}^2 \quad (2)$$

where h represents the center of equally spaced-bins having a lag equal to 2δ In Equation (2), each experimental point $\gamma(h_k)$, for each distance bin h_k, is obtained through the average of the quadratic differences among the experimental measurements. It is verified that for the stationary dataset, this estimator tends to the dataset variance. In this context, we offer a new method for the creation of interpolated maps (kriging) based on the Gini index [28,29] to characterize the distribution of Rn concentration. According to Loffredo et al., 2021, it is a best practice to undertake data processing to ensure the hypothesis of stationarity (ergodicity).

The Gini-based semivariogram is shown below, and it is based on the Gini index, which is defined as:

$$\gamma_G(h_k) = \left[\frac{1}{n-1}\sum_{i=1}^{n}|z(x_i) - \mu|^2\right]\frac{1}{n_{G_k}}\sum_{j=1}^{n_{G_k}}\frac{G_{jk}}{mean(G)} \quad (3)$$

where n is the number of experimental measurements, $z(x_i)$ are the values of the variable in their geographic location, μ is the mean of the entire dataset and hence the first factor at the second member is the sample variance of the dataset [28,29]. The index j denotes the available Gini coefficients in the column G_{jk}, and G denotes all of the values in the matrix G_i.

In Equation (3) the variogram is factorized; the absolute variability of the dataset distribution is accounted through the calculation of the variance, while the relative spatial inhomogeneity, describing the spatial correlation of the dataset, is instead taken into account by means of average Gini indices. Therefore, whether this quantity tends to a plateau level, $\gamma_G(h_k)$ will tend to the dataset variance equivalently to the classical semi-variogram.

This strategy appears to be useful for identifying large-scale spatial connections that can then be linked to geological phenomena. This is particularly intriguing because assessing and minimizing the danger of radon exposure necessitates determining local geology and its relationship to radon exhalation.

4. Results and Discussion

The measurement survey at the 96 houses in Kpong was made possible thanks to the voluntary participation of the inhabitants of the area. From the indoor radon measurements conducted at the homes we obtained the following main results, as shown in Table 1.

Table 1. Statistical parameters (arithmetic mean (AM), the geometric mean (GM), the standard deviation (SD), the coefficient of variation (CV), the geometric standard deviation (GSD), the minimum (Min), the median (Med) and the maximum (Max)) for the total measurements on the Kpong.

Statistical Parameters	Kpong
AM (Bq/m^3)	55
SD (Bq/m^3)	36
CV = SD/AM	0.65
GM (Bq/m^3)	43
GSD (Bq/m^3)	1.37
Min (Bq/m^3)	4
Med (Bq/m^3)	44
Max (Bq/m^3)	176

The survey indicated that the concentrations range from 4 Bq^{-3}–176 Bqm^{-3}. The data showed that 84% of the residences monitored had radon levels below 100 Bqm^{-3} that is the WHO's suggested reference range [35] and the mean value 55 Bqm^{-3} is 38% higher than the world's average IRC of 40Bqm^{-3} [36]. This could be due to the composition of the bedrock (schists, quartzite and phyllites, unaltered schists and sandstone). The Loffredo et al. 2021 [30] survey conducted in the Sorrento Peninsula, Italy, found indoor radon concentrations in dwellings higher than these results. Also, in the Adelikhah et al., 2021 work [20] conducted in dwellings in Mashhad, Iran, indoor radon concentrations in dwellings were higher than our results. In the Yarmoshenko et al. study [37] specifically to the city of Nizhny Novgorod in Russia, the indoor radon concentrations in dwellings showed a lower radon concentration than that obtained in the present study. Finally, in Yeboah, [32], an indoor radon concentration similar to that obtained in the present study was shown.

Figure 4a,b shows the frequency distribution of the indoor radon concentration and Q-norm plot of natural log-transformed radon concentrations in 96 dwellings in Kpong. The experimental data follow a log-normal distribution. The log-normal trend was confirmed with the Kolmogorov-Smirnov test ($p > 0.05$, 95% confidence level).

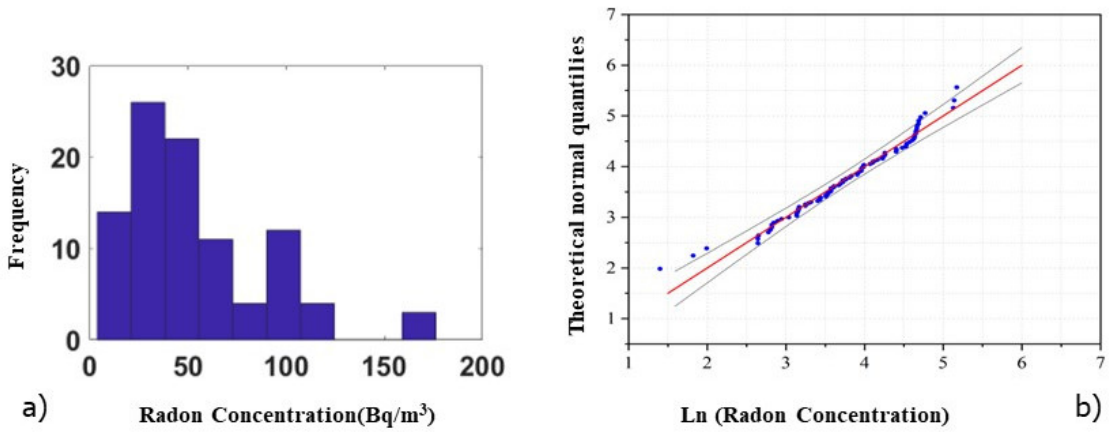

Figure 4. (**a**) Frequency distribution of indoor radon concentrations measured in dwellings in Kpong; (**b**) Q-norm plot of natural log-transformed radon concentration, reference line in red, lower, and upper percentile in black.

It is well known in the literature that the indoor radon concentrations are generally affected by several factors such as building materials. To analyze the influence of building

materials, the monitored homes were grouped in two categories: (i) cement and blocks; and (ii) mud plastered with cement. Based on the result of the *t*-test, the significant difference in the annual average radon concentrations between two different building materials was not observed ($p = 0.37$). The variation of radon concentration with respect to the different building materials is reported in the box plot of Figure 5.

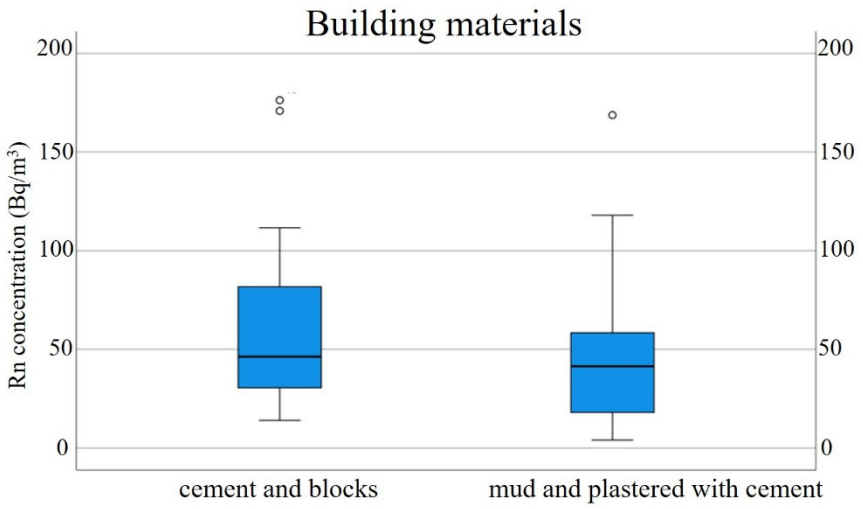

Figure 5. Relationship between radon concentrations and building materials. The graph reports the median and 25th and 75th percentiles; the outlier values are represented by circles.

The spatial autocorrelation study was performed with the Gini-based variogram, as shown in Figure 6, after the verification of the quasi-stationary model with the classical variogram.

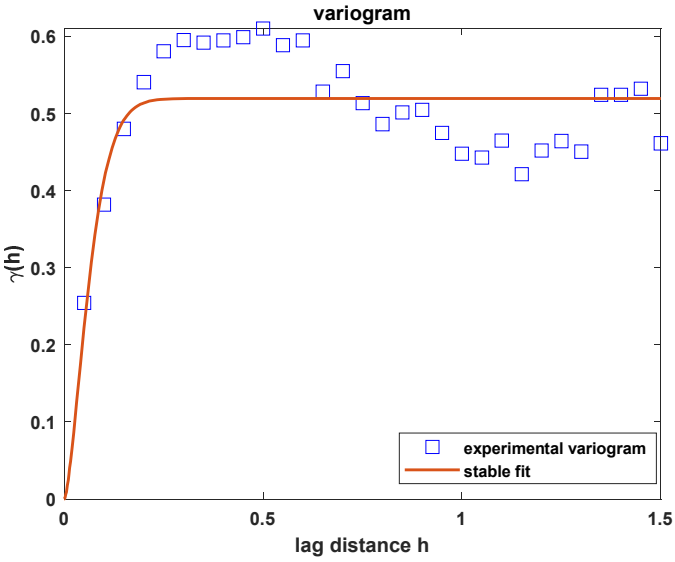

Figure 6. Experimental variogram (blue squares) based on the Gini index for 96 measurement points that were modelled by a stable function (red line).

The variogram γ (h) tends to zero when h tends to zero. In this case, a relevant nugget effect cannot be identified. Generally, the presence of the nugget effect is expected in cases of quantities relating to Rn, however in the specific case, the absence of this effect could be due to measurements of uncertainty low on measurements at small distances. Given the size of the investigated area, the amount of data supplied can be regarded as sufficient for the study.

The geostatistical analysis of the data indicates the existence of a spatial correlation, and the variogram has been modelled by this function.

$$\gamma(h) = S \cdot \left[1 - \exp\left(-\frac{h}{R}\right)^{\alpha}\right] + N \quad (4)$$

The range (R) is the distance at which the semi-variogram gets about the 63% of the plateau level. This plateau level is given by the sum of the sill (S) parameter, indicating the physically-based spatial variability of the whole dataset and the nugget (N) that describes the variability level due to the random uncertainty of the dataset. In the specific case α = 1.5 [28], a sill of 0.18, a range of 0.87 km.

The variogram's trend has been demonstrated up to a distance of ~1 km, for which spatial correlation is assured. In the Gini-based approach, the variogram is computed by clustering a larger number of experimental data. As a consequence, the single measurements, possibly affected by a large random uncertainty, are weighted less.

Figure 7 shows the geographical distribution of radon concentrations in the Kpong area. The kriging map describes an area that does not show a significant correlation between the measures, and this can be seen from the variogram, which provides a low range value. This implies that no spatial correlation is present at distances greater than 0.87 km. At the lower left corner, in Figure 7, the presence of an anomalous radon source cannot be guaranteed due to the lack of data in the neighboring area. In this work it was not possible to carry out a correlation study with geology due to the lack of data describing the geological composition of the monitored region. In the future, when the geolithological maps of the region are available, the interpolated maps will be superimposed on them.

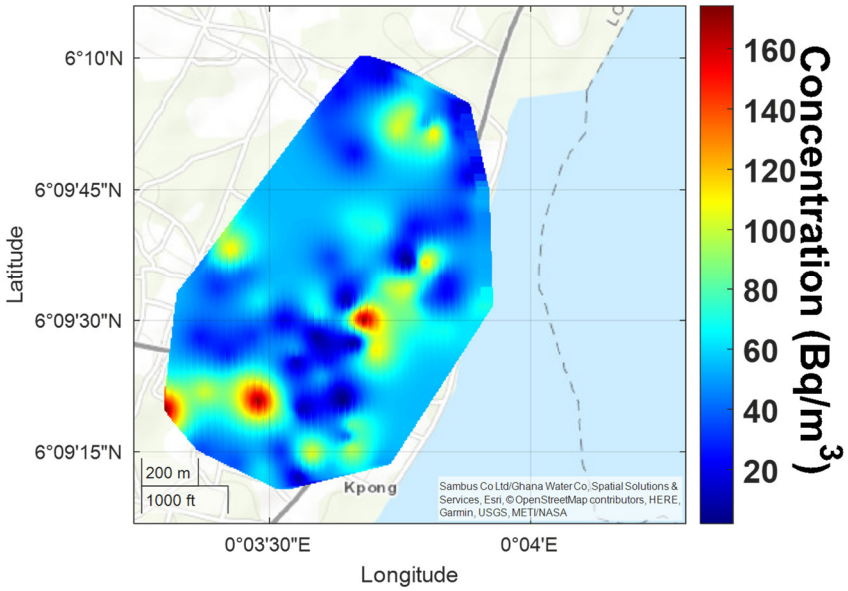

Figure 7. Kriging map obtained with the Gini method for 96 measurement points on the Kpong, Ghana.

Results shown in several studies and performed in different parts of the world have shown that radon distribution is closely related to geology, the presence of faults, local lithology, and the distribution of ^{238}U in soil. In particular, the latter feature is the main result obtained in many works aimed at mapping the potential of radon in an investigated area [21,27,38]. In addition, a relationship between the geogenic potential of radon and indoor concentrations has been shown [39,40]. To verify the correlation between indoor radon concentration and geogenic potential radon, the dependence on the floor should be eliminated by normalizing the data [30,41]. Finally, other studies have confirmed how the

intensive use of some building materials with high concentrations of ^{232}Th, ^{226}Ra and ^{40}K increase the risk of radon potential [22,42].

5. Conclusions

The indoor radon concentrations were measured in 96 dwellings of the Kpong area in Ghana. The radon concentration values ranged from 4 Bq^{-3} to 176 Bq m^{-3}. Comparing the current study to a work conducted at Aburi (51.4 km from Kpong) and in the same region (Eastern region of Ghana) recorded ~50 Bqm^{-3} which is quite close to the mean of this study (55 ± 36 Bqm^{-3}) [32]. This might be due to the common bedrock formation of these two study areas. The Togo formations (schists, quartzite and phyllites, unaltered shale and sandstone) are rocks forming the Akwapim range of hills trending northeast from the coast West of Accra through Kpong, Aburi, and Anum into the Republic of Togo [30]. The kriging map was made using the Gini method and estimated using the geographic distribution of the measurement points over the Kpong area. The created geographical map of the indoor radon concentrations in dwellings of Kpong did not indicate any clear pattern but contributes spatially to our understanding of indoor radon distribution at Kpong. The map represents an estimate of the global distribution of Rn indoor concentrations. This could be a good starting point for obtaining a radon distribution map over larger areas. Currently, the Ghana Atomic Energy Commission and the Ghana Environmental Protection Agency are working assiduously to come out with a reference level for indoor radon in Ghana since there is currently no national average for radon levels in dwellings.

Author Contributions: Conceptualization, F.L., I.O.-N. and M.Q.; methodology, F.L., I.O.-N. and M.Q.; software, F.L. and I.O.-N.; validation, F.L. and I.O.-N.; formal analysis, F.L., I.O.-N. and D.K.-M.; investigation, F.L., I.O.-N. and D.K.-M.; resources, F.L., I.O.-N., D.K.-M. and M.Q.; data curation, F.L., I.O.-N., D.K.-M. and M.Q.; writing—original draft preparation, F.L., I.O.-N., D.K.-M. and M.Q.; writing—review and editing, F.L., I.O.-N., D.K.-M. and M.Q.; visualization, F.L., I.O.-N., D.K.-M. and M.Q.; supervision, M.Q.; project administration, M.Q.; funding acquisition, F.L., I.O.-N. and M.Q. All authors have read and agreed to the published version of the manuscript.

Funding: This research has been partially supported by the Italian Ministry of University and Research (MIUR), within the program PON R&I 2014-2020- Attraction and International Mobility (AIM)- CUP E61G19000020001.

Institutional Review Board Statement: Not applicable.

Informed Consent Statement: Not applicable.

Data Availability Statement: The data presented in this study are available on request from the corresponding author. The data are not publicly available due to the non-exclusive ownership by the authors.

Conflicts of Interest: The authors declare no conflict of interest.

References

1. Collier, C.G.; Strong, J.C.; Humphreys, J.A.; Timpson, N.; Baker, S.T.; Eldred, T.; Cobbi, L.; Papworth, D.; Haylock, R. Carcinogenicity of radon/radon decay product inhalation in rats—Effect of dose, dose rate and unattached fraction. *Int. J. Radiat. Biol.* **2005**, *81*, 631–647. [CrossRef] [PubMed]
2. Righi, S.; Verità, S.; Albertazzi, A.; Rossi, P.L.; Bruzzi, L. Natural radioactivity in refractory manufacturing plants and exposure of workers to ionising radiation. *J. Environ. Radioact.* **2009**, *100*, 540–546. [CrossRef] [PubMed]
3. Loffredo, F.; Vardaci, E.; Roca, V.; Pugliese, M. Space missions: Comparison of shielding effectiveness among different materials using 1 GeV protons. *Mater. Res. Express* **2019**, *6*, 016544. [CrossRef]
4. Quarto, M.; Pugliese, M.; Loffredo, F.; La Verde, G.; Roca, V. Indoor radon activity concentration measurements in the great historical museums of University of Naples, Italy. *Radiat. Prot. Dosim.* **2016**, *168*, 116–123. [CrossRef] [PubMed]
5. Quarto, M.; Pugliese, M.; Loffredo, F.; Zampella, C.; Roca, V. Radon measurements and effective dose from radon inhalation estimation in the neapolitan catacombs. *Radiat. Prot. Dosim.* **2014**, *158*, 442–446. [CrossRef]
6. Caridi, F.; Marguccio, S.; Belvedere, A.; D'Agostino, M. Validation of gamma-ray spectrometry (GRS) for radionuclides analysis of environmental and food samples. *Appl. Sci.* **2019**, *1*, 256. [CrossRef]

7. Environmental Protection Agency (EPA). *EPA Assessment of Risks from Radon in Homes*; Office of Radiation and Indoor Air. United States Environmental Protection Agency: Washington, DC, USA, 2003. Available online: https://www.epa.gov/sites/default/files/2015-05/documents/402-r-03-003.pdf (accessed on 1 June 2022).
8. Wilson, J.W.; Mertens, C.J.; Goldhagan, P.; Friedberg, W.; De Angelis, G.; Clem, J.M.; Copeland, K.; Bidasaria, H.B. Atmospheric ionizing radiation and human exposure. *NASA Tech. Rep.* **2005**. NASA/TP-2005-213935. Available online: https://spaceradiation.larc.nasa.gov/nasapapers/2005/20050237978.pdf (accessed on 1 June 2022).
9. Mertens, C.J.; Kress, B.T.; Wiltberger, M.; Tobiska, W.K.; Grajewski, B.; Xu, X. *Atmospheric Ionizing Radiation from Galactic and Solar Cosmic Rays, 2012 in Current Topics in Ionizing Radiation Research*; Nenoi, M., Ed.; InTech: Rijeka, Croatia, 2019; ISBN 978-953-51-0196-3.
10. Bochicchio, F.; Forastiere, F.; Farchi, S.; Quarto, M.; Axelson, O. Residential radon exposure, diet and lung cancer: A case-control study in a Mediterranean region. *Int. J. Cancer* **2005**, *114*, 983–991. [CrossRef]
11. Darby, S.; Hill, D.; Auvinen, A.; Barros-Dios, J.M.; Baysson, H.; Bochicchio, F.; Deo, H.; Falk, R.; Forastiere, F.; Hakama, M.; et al. Radon in homes and lung cancer risk: Collaborative analysis of individual data from 13 European case-control studies. *Br. Med. J.* **2005**, *330*, 223–226. [CrossRef]
12. Krewski, D.; Lubin, J.H.; Zielinski, J.M.; Alavanja, M.; Catalan, V.S.; Field, R.W.; Klotz, J.B.; Le'Tourneau, E.G.; Lynch, C.F.; Lyon, J.I.; et al. Residential radon and risk of lung cancer: A combined analysis of 7 north american case-controls studies. *Epidemiology* **2005**, *16*, 137–145. [CrossRef]
13. Krewski, D.; Lubin, J.H.; Zielinski, J.M.; Alavanja, M.; Catalan, V.S.; Field, R.W.; Klotz, J.B.; Le'Tourneau, E.G.; Lynch, C.F.; Lyon, J.L.; et al. A combined analysis of North American case–control studies of residential radon and lung cancer. *J. Toxicol. Environ. Health A* **2006**, *69*, 533–597. [CrossRef] [PubMed]
14. Garzillo, C.; Pugliese, M.; Loffredo, F.; Quarto, M. Indoor radon exposure and lung cancer risk: A meta-analysis of case-control studies. *Transl. Cancer Res.* **2017**, *6*, S934–S943. [CrossRef]
15. Lubin, J.H.; Wang, Z.Y.; Boice, J.D.J.; Zhao, Y.X.; Blot, W.J.; De Wang, L.; Kleinerman, R.A. Risk of lung cancer and residential radon in China: Pooled results of two studies. *Int. J. Cancer* **2004**, *109*, 132–137. [CrossRef] [PubMed]
16. UNSCEAR (United Nations Scientific Committee on the Effects of Atomic Radiation). *Sources and Effects of Ionizing Radiation. Report to the General Assembly*; United Nations: New York, NY, USA, 2000.
17. Kitson-Mills, D.; Sovoe, S.; Opoku-Ntim, I.; Kyei, K.A.; Marnotery, S.; Anim-Sampong, S.; Kwabeng, M.A.; Otoo, F.; Baiden, F. An assessment of indoor radon level in a suburb of Ghana. *Environ. Res. Commun.* **2019**, *1*, 061002. [CrossRef]
18. Opoku-Ntim, I.; Andam, A.B.; Roca, V.; Fletcher, J.J.; Akiti, T.T. Indoor radon concentration and risk assessment in some dwellings of Obuasi, Mining Town. *Radiat. Prot. Dosim.* **2020**, *188*, 30–37. [CrossRef]
19. Webster, R.; Oliver, M.A. *Geostatistics for Environmental Scientists*, 2nd ed.; John Wiley & Sons: Chichester, UK, 2007.
20. Adelikhah, M.; Shahrokhi, A.; Imani, M.; Chalupnik, S.; Kovács, T. Radiological Assessment of Indoor Radon and Thoron Concentrations and Indoor Radon Map of Dwellings in Mashhad, Iran. *Int. J. Environ. Res. Public Health* **2021**, *18*, 141. [CrossRef]
21. Sabbarese, C.; Ambrosino, F.; D'Onofrio, A.; Pugliese, M.; La Verde, G.; D'Avino, V.; Roca, V. The first radon potential map of the Campania region (southern Italy). *J. Appl. Geochem.* **2021**, *126*, 104890. [CrossRef]
22. Giustini, F.; Ciotoli, G.; Rinaldini, A.; Ruggiero, L.; Voltaggio, M. Mapping the geogenic radon potential and radon risk by using Empirical Bayesian Kriging regression: A case study from a volcanic area of central Italy. *Sci. Total Environ.* **2019**, *661*, 449–464. [CrossRef]
23. Lima, A.; De Vivo, B.; Cicchella, D.; Cortini, M.; Albanese, S. Multifractal IDW interpolation and fractal filtering method in environmental studies: An application on regional stream sediments of (Italy), Campania region. *Appl. Geochem.* **2003**, *18*, 1853–1865. [CrossRef]
24. Borgoni, R.; Quatto, P.; Somà, G.; De Bartolo, D. A geostatistical approach to define guidelines for radon prone area identification. *J. Ital. Stat. Soc.* **2009**, *19*, 255–276. [CrossRef]
25. Bossew, P.; Žunić, Z.; Stojanovska, Z.; Tollefsen, T.; Carpentieri, C.; Veselinović, N.; Komatina, S.; Vaupotič, J.; Simović, R.; Antignani, S.; et al. Geographical distribution of the annual mean radon concentrations in primary schools of Southern Serbia-Application of geostatistical methods. *J. Environ. Radioact.* **2014**, *127*, 141–148. [CrossRef] [PubMed]
26. Cafaro, C.; Bossew, P.; Giovani, C.; Garavaglia, M. Definition of radon prone areas in Friuli Venezia Giulia region, Italy, using geostatistical tools. *J. Environ. Radioact.* **2014**, *138*, 208–219. [CrossRef] [PubMed]
27. Ciotoli, G.; Voltaggio, M.; Tuccimei, P.; Soligo, M.; Pasculli, A.; Beaubien, S.; Bigi, S. Geographically weighted regression and geostatistical techniques to construct the geogenic radon potential map of the Lazio region: A methodological proposal for the European Atlas of Natural Radiation. *J. Environ. Radioact.* **2017**, *166*, 355–375. [CrossRef]
28. Loffredo, F.; Scala, A.; Adinolfi, G.M.; Savino, F.; Quarto, M. A new geostatistical tool for the analysis of the geographical variability of the indoor radon activity. *Nukleonika* **2020**, *65*, 99–104. [CrossRef]
29. Loffredo, F.; Scala, A.; Serra, M.; Quarto, M. Radon risk mapping: A new geostatistical method based on Lorenz Curve and Gini index. *J. Environ. Radioact.* **2021**, *233*, 106612. [CrossRef] [PubMed]
30. Loffredo, F.; Opoku-Ntim, I.; Quarto, M. Sorrentina Peninsula: Geographical Distribution of the Indoor Radon Concentrations in Dwellings—Gini Index Application. *Appl. Sci.* **2021**, *11*, 7975. [CrossRef]
31. Otoo, F.; Arhin, I.; Darko, E.O. Studies of Radon Levels, Radium Concentration, and Estimated Effective Dose in Dwellings and Soils in Gold Mining Towns in Abirem of Eastern Region of Ghana. *Radiat. Prot. Dosim.* **2020**, *191*, 296–309. [CrossRef]

32. Yeboah, S.M. Indoor Radon in Selected Homes in Aburi Municipality: Measurement Uncertainty, Decision Analysis and Remediation Strategy. Ph.D. Dissertation, University of Ghana, Accra, Ghana, 2014.
33. Ghana Statistical Service (GSS). Population and Housing Census Final Report. Printed by Sakoa, Accra; 2010. Available online: https://www.statsghana.gov.gh/gssmain/storage/img/marqueeupdater/Census2010_Summary_report_of_final_results.pdf (accessed on 29 April 2022).
34. Amponsah, P.E. Seismic activity in relation to fault systems in southern Ghana. *J. Afr. Earth Sci.* **2002**, *35*, 227–234. [CrossRef]
35. World Health Organization. *WHO Handbook on Radon: A Public Health Perspective*; Hajo, Z., Ferid, S., Eds.; World Health Organization: Geneva, Switzerland, 2009; pp. 1–94.
36. UNSCEAR (United Nations Scientific Committee on the Effects of Atomic Radiation). *Sources and Effects of Ionizing Radiation, Report to the General Assembly, with Scientific Annexes*; United Nation: New York, NY, USA, 1993.
37. Yarmoshenko, I.; Malinovsky, G.; Vasilyev, A.; Onishchenko, A. Seasonal Variation of Radon Concentrations in Russian Residential High-Rise Buildings. *Atmosphere* **2021**, *12*, 930. [CrossRef]
38. Liu, H.; Wang, N.; Chu, X.; Li, T.; Zheng, L.; Yan, S.; Li, S. Mapping radon hazard areas using 238U measurements and geological units: A study in a high background radiation city of China. *J. Radioanal. Nucl. Chem.* **2016**, *309*, 1209–1215. [CrossRef]
39. Kemski, J.; Klingel, R.; Siehl, A.; Valdivia-Manchego, M. From radon hazard to risk prediction based on geological maps, soil gas and indoor measurements in Germany. *Environ. Geol.* **2009**, *56*, 1269–1279. [CrossRef]
40. Nuhu, H.; Hashim, S.; Aziz Saleh, M.; Syazwan Mohd Sanusi, M.; Hussein Alomari, A.; Jamal, M.H.; Abdullah, R.A.; Hassan, S.A. Soil gas radon and soil permeability assessment: Mapping radon risk areas in Perak State, Malaysia. *PLoS ONE* **2021**, *16*, e0254099. [CrossRef] [PubMed]
41. Giustini, F.; Ruggiero, L.; Sciarra, A.; Beaubien, S.E.; Graziani, S.; Galli, G.; Pizzino, L.; Tartarello, M.C.; Lucchetti, C.; Sirianni, P.; et al. Radon Hazard in Central Italy: Comparison among Areas with Different Geogenic Radon Potential. *Int. J. Environ. Res. Public Health* **2022**, *19*, 666. [CrossRef] [PubMed]
42. Coletti, C.; Ciotoli, G.; Benà, E.; Brattich, E.; Cinelli, G.; Galgaro, A.; Massironi, M.; Mazzoli, C.; Mostacci, D.; Morozzi, P.; et al. The assessment of local geological factors for the construction of a Geogenic Radon Potential map using regression kriging. A case study from the Euganean Hills volcanic district (Italy). *Sci. Total Environ.* **2021**, *808*, 152064. [CrossRef]